Biogeosciences Discuss., https://doi.org/10.5194/bg-2018-37
Manuscript under review for journal Biogeosciences
Discussion started: 31 January 2018

Carbon Dioxide and Methane Emissions from Red Sea Mangrove Sediments

Mallory A. Sea[1], Neus Garcias-Bonet[1], Vincent Saderne[1]* and Carlos M. Duarte[1]

[1] {King Abdullah University of Science and Technology (KAUST), Red Sea Research Center (RSRC), Thuwal, 23955-6900, Saudi Arabia}

*Correspondence to: V. Saderne (vincent.saderne@kaust.edu.sa)

Abstract

Mangrove forests are highly productive tropical and subtropical coastal systems that provide a variety of ecosystem services, including the sequestration of carbon. While mangroves are reported to be the most intense carbon sinks among all forests, their sediments can also support large emissions of greenhouse gases (GHG), such as carbon dioxide (CO_2) and methane (CH_4), to the atmosphere. However, data derived from arid mangrove systems like the Red Sea are lacking. Here, we report emission rates of CO_2 and CH_4 from mangrove sediments along the Saudi Arabian coast of the Red Sea, and assess the relative role of these two gases in supporting total GHG emissions. Diel CO_2 and CH_4 emission rates in Red Sea mangrove sediments ranged from -3452 to 7500 µmol CO_2 m^{-2} d^{-1} and from 0.9 to 13.3 µmol CH_4 m^{-2} d^{-1}, respectively. The rates reported here fall within previously reported ranges for both CO_2 and CH_4, but maximum CO_2 and CH_4 flux rates in the Red Sea are 10 to 100-fold below those previously reported for mangroves elsewhere. Based on the isotopic composition of the CO_2 and CH_4 produced by mangrove sediments, we identified the origin of the organic matter that supports GHG emissions. In most of the mangrove stands, GHG emissions were supported by organic matter from mixed

sources while only in one mangrove stand the GHG emissions were supported by organic matter derived from mangrove tissues. Moreover, the organic matter derived from mangrove tissues reduced CO_2 fluxes and enhanced CH_4 production, pointing out the importance of the origin of the organic matter in GHG emissions. Methane was the main source of CO_2-equivalents, despite the comparatively low emission rates, in most of the sampled mangroves, and therefore deserves careful monitoring in this region. Despite the mean net emission of CO_2 and CH_4 by Red Sea mangroves reported here, these forests become net organic carbon sinks when taking into account the existing carbon burial rates for the Red Sea mangroves. By further resolving GHG fluxes in arid mangroves, we will better ascertain the role of these forests in global carbon budgets.

Biogeosciences Discuss., https://doi.org/10.5194/bg-2018-37
Manuscript under review for journal Biogeosciences
Discussion started: 31 January 2018

1 Introduction

Mangrove forests, typically growing in the intertidal zones of tropical and subtropical coasts, are highly productive components of coastal ecosystems and adapted to high salinity and anoxic conditions associated with waterlogged sediments. Mangrove forests cover a global estimated area of 137,760 km^2 (Giri et al., 2011) and are typically constrained by temperature, with greatest biomass and species diversity in the equatorial zone (Alongi, 2012). Mangroves rank amongst the most threatened ecosystems in the biosphere, with losses estimated at 50% of their global extent over the past 50 years (Giri et al., 2011). These losses affect all mangrove regions, except for the Red Sea, where mangrove coverage has increased by 13% over the past four decades (Almahasheer et al., 2016).

Loss of mangrove forest represents a loss of valuable ecosystem services, including habitat and nursery for marine species, coastal protection from erosion due to wave action, and the filtration of harmful pollutants from terrestrial sources (Alongi, 2008), as well as loss of CO_2 sink capacity and a source of emissions of greenhouse gases (GHG) from disturbed soil carbon stocks (Donato et al., 2011; Alongi, 2014). Hence, mangrove conservation and restoration have been proposed as important components of so-called Blue Carbon strategies to mitigate climate change (Duarte, et al., 2013). Indeed, mangroves are reported to be the most intense carbon sinks among all forests, supporting carbon sequestration rates and organic carbon stocks as much as five times higher than those in terrestrial forests (Donato et al., 2011). While mangrove forests cover less than 1% of total coastal ocean area, they contribute to almost 15% of total carbon sequestration in coastal ecosystems (Alongi, 2012), making mangrove forests highly effective in terms of carbon sequestration per unit area. The management of mangroves to maximize CO_2 removal and subsequent storage is gaining momentum as a cost-effective strategy to mitigate climate change.

However, mangroves act as both carbon sinks and sources, as their sediments have been reported to support large GHG emissions, in the forms of CO_2 and CH_4 (Allen et al., 2007; Kristensen et al., 2008a; Chen et al., 2016). Whereas concerns are focused on GHG emissions following

mangrove disturbance, estimated at 0.02 – 0.12 Pg C yr^{-1} globally (Donato et al., 2011), undisturbed mangrove sediments also support GHG emissions (Purvaja and Ramesh, 2000; Kristensen et al., 2008b; Chauhan et al., 2015). Previous studies on GHG emission rates from mangrove sediments show highly variable fluxes, with mangroves reported to act from negligible (Alongi, 2005) to considerable sources (Livesley and Andrusiak, 2012; Chen et al., 2016). Comparisons of carbon sequestration rates between mangrove stands have revealed that climatic conditions play an important role, with mangroves in the arid tropics, such as those in the Red Sea, supporting the lowest carbon sequestration rates (Almahasheer et al. 2017). Likewise, GHG emissions from mangrove forests may vary with climate, with most reported rates to-date derived from the wet tropics (Alongi et al., 2005; Chauhan et al., 2015; Chen et al., 2016). Whereas Red Sea mangroves are considered to play a minor role as CO_2 sinks, their role may be greater than portrayed by low carbon burial rates if they also support very low GHG emissions, thereby leading to a balance comparable to mangroves in the wet tropics.

Here we report emission rates of CO_2 and CH_4, along with their carbon isotopic composition, from mangrove sediments along the Saudi coast of the Red Sea, and assess the relative role of these two gases in supporting total GHG emissions as well as their fluctuations along the day-night cycle.

2 Materials and Methods

2.1 Study area

We sampled seven mangrove forests along the eastern coast of the Red Sea (Fig. 1). We collected triplicate sediment cores (translucent PVC tubes, 30.5 cm in height and 9.5 cm in diameter) at each station in order to measure CO_2 and CH_4 fluxes. Additionally, we analyzed sediment chlorophyll *a* and nutrient (organic carbon and nitrogen) content. Mangrove sediments were sampled five to ten meters from the forest edge, typically in the center of the mangrove belt. We sampled two stations (S1 and S2) in January and February 2017 and the other five mangrove stations (S3-S7) in March on board the R/V Thuwal as part of a scientific cruise. The sediment cores collected from S1 and S2 were immediately transported to the laboratory and

placed in seawater baths and enclosed in environmental growth chambers (Percival Scientific Inc., Perry, IA, USA) with 12h-light:12h-dark cycles at a constant temperature of 26°C. The sediment cores collected during the scientific cruise were transported immediately on board and placed in open aquarium tanks with running seawater in order to keep them close to *in situ* temperature. Salinity and temperature were routinely recorded using a CTD.

2.2 Sediment characteristics

The chlorophyll *a* content of the sediment was measured by fluorometry. The surface layer of each replicate core was collected and frozen until further analysis. Prior to chlorophyll *a* extraction, the sediment samples were left at room temperature to thaw. The chlorophyll *a* was extracted by adding 7 ml of 90% acetone to 2 ml of sediment sample. After a 24h incubation at 4° C in dark conditions, the samples were centrifuged and the chlorophyll *a* content in the supernatant was measured on a Trilogy fluorometer. The nutrient (organic carbon and nitrogen) content of the sediment was analyzed on an Organic Elemental Analyzer (Flash 2000) after acidification of sediment samples.

2.3 Measurement of greenhouse gas fluxes

We measured CO_2 and CH_4 fluxes in mangrove sediments using two different techniques. The CO_2 and CH_4 fluxes from S1 and S2 were measured using the closed water circuit technique and the CO_2 and CH_4 fluxes from the rest of the stations sampled during the scientific cruise (S3-S7) were measured using the headspace technique.

2.3.1 Measurement of CO_2 and CH_4 fluxes in sediment core incubations using closed water circuit technique

Biogeosciences Discuss., https://doi.org/10.5194/bg-2018-37
Manuscript under review for journal Biogeosciences
Discussion started: 31 January 2018

We incubated mangrove sediment cores from stations S1 and S2 using a closed water circuit technique in order to measure changes in CO_2 and CH_4 concentrations. Before starting the incubation, the seawater above the sediment from each core was replaced by fresh seawater collected from the same location, avoiding disturbance of the sediment. Then, the seawater from the core was recirculated by a peristaltic pump in an enclosed water circuit through a membrane equilibrator (Liqui-cel mini module, 3M, Minnesota, USA). This setup enables the equilibration of gases in dissolution with an enclosed air circuit. The air from the enclosed air circuit was then passed through a desiccant (calcium sulfate, WA Hammond Drierite Co., LTD, Ohio, USA) column and flowed into a cavity ring-down spectrometer (CRDS; Picarro Inc., Santa Clara, CA, USA) to continuously measure the CO_2 and CH_4 concentration. We ran the incubations for at least 30 minutes under light (200 µmol photons m^{-2} s^{-1}) and dark conditions.

The concentration of CO_2 in the water circuit (µmol ml^{-1}) was calculated by Eq. (1):

$$[CO_2] = Hcp \times [HP\_CO_2] \times (1 - pH_20), \quad (1)$$

where Hcp is the Henry constant (mol ml^{-1} atm^{-1}) calculated using R marelac package (Soetaert et al., 2016); $[HP\_CO_2]$ is the given concentration of CO_2 (ppm), and pH_20 is the water vapor pressure (atm).

The CO_2 fluxes were calculated from the change in CO_2 concentration over time during our incubations, correcting by the seawater volume present in each core. Then, the fluxes were transformed to an aerial basis (µmol m^{-2} h^{-1}) by taking into account the core surface area. Finally, the daily fluxes (µmol m^{-2} d^{-1}) were calculated by multiplying the CO_2 flux obtained under light conditions by the number of light hours plus the CO_2 flux obtained under dark conditions by the number of dark hours.

The CH_4 fluxes were calculated in the same manner as for the CO_2 fluxes, with the exception that the Henry constant was calculated using Eq. (2):

$$\beta = Hcp \times (RT), \quad (2)$$

Biogeosciences Discuss., https://doi.org/10.5194/bg-2018-37
Manuscript under review for journal Biogeosciences
Discussion started: 31 January 2018

where Hcp is the Henry constant (mol ml^{-1} atm^{-1}), R is the ideal gas constant (82.057338 atm ml mol^{-1} K^{-1}), T is standard temperature (273.15 K), and β is the Bunsen solubility coefficient of CH_4, extracted from Wiesenburg and Guinasso (1979).

2.3.2 Measurement of CO_2 and CH_4 fluxes in sediment core incubations using the headspace technique

Mangrove sediment cores from stations S3 to S7 were incubated using a headspace technique in order to measure changes in CO_2 and CH_4 concentrations. Before starting the incubation, the seawater above the sediment from each core was replaced by fresh seawater from the running seawater system, leaving a headspace of 200 ml. Each core was sealed with a stopper equipped with a gas-tight valve serving as a headspace sampling port. The sealed core was left for 1 hour before the first headspace sampling to allow equilibration between seawater and air phases. Each core was sampled with a syringe, withdrawing 15 ml of air from the equilibrated headspace. Headspace samples were periodically drawn from each sediment incubation over a 24-hour incubation period. The CO_2 and CH_4 concentrations in the headspace samples along with their isotopic composition ($\delta^{13}C$-CO_2 and $\delta^{13}C$-CH_4) were measured with a cavity ring-down spectrometer (CRDS; Picarro Inc., Santa Clara, CA, USA) connected to a small sample isotopic module extension (SSIM A0314, Picarro Inc., Santa Clara, CA, USA). We ran standards (730 ppm CO_2, 1.9 ppm CH_4) before and after every three samples.

The concentration of dissolved CO_2 in the seawater after equilibrium was calculated from the concentration in the equilibrated headspace (ppm) as described previously by Wilson et al. (2012) for other gases:

$$[CO_2]_w = 10^{-6} \beta m_a p_{dry}, \quad (3)$$

where β is the Bunsen solubility coefficient of CO_2 (mol ml^{-1} atm^{-1}), m_a is the given concentration of CO_2 in the equilibrated headspace (ppm), and p_{dry} is atmospheric pressure (atm) of dry air. The Bunsen solubility coefficient of CO_2 was calculated using Eq. (4):

$$\beta = Hcp \times (RT) \quad (4)$$

where Hcp is the Henry constant (mol ml^{-1} atm^{-1}) calculated using R marelac package (Soetaert et al., 2016), R is the ideal gas constant (82.057338 atm ml mol^{-1} K^{-1}) and T is standard temperature (273.15 K). The atmospheric pressure of dry air (p_{dry}) was calculated using Eq. (5):

$$p_{dry} = p_{wet} (1 - \%H_20) \quad (5)$$

where p_{wet} is the atmospheric pressure of wet air corrected by the effect of multiple syringe draws from the same core, applying Boyle's law.

The initial concentration of dissolved CO_2 in seawater before equilibrium was then calculated as:

$$[CO_2]_{aq} = ([CO_2]_w V_w + 10^{-6} m_a V_a) / V_w \quad (6)$$

where $[CO_2]_w$ is the concentration of dissolved CO_2 in the seawater after equilibrium, V_w is the volume of seawater (ml) and V_a is the headspace volume (ml) in the core. Finally, treating the gas as ideal, the units were converted to nM using Eq. (7):

$$[CO_2]_{aq} = 10^9 * p_{dry}[CO_2]_{aq} / (RT) \quad (7)$$

where R is the ideal gas constant (0.08206 atm l mol^{-1} K^{-1}) and T is temperature (K).

The CO_2 fluxes were calculated from the change in CO_2 concentration over time during our incubations, correcting by the seawater volume present in each core. Then, the fluxes were transformed to an aerial basis (µmol m^{-2} d^{-1}) by taking into account the core surface area. Finally, the day and night fluxes (µmol m^{-2} h^{-1}) were calculated from the change in CO_2 concentration between consecutive samplings during day and night time, respectively.

The CH_4 fluxes were calculated in the same manner as for the CO_2 fluxes, with the exception that the Bunsen solubility coefficient of CH_4 was calculated according to Wiesenburg and Guinasso (1979).

2.4 Isotopic composition of CO_2 ($\delta^{13}C$- CO_2) and CH_4 ($\delta^{13}C$- CH_4)

192 The isotopic signature of the CO_2 and CH_4 produced in the sediment incubations was estimated
193 by conducting keeling plots (Pataki et al. 2003; Thom et la. 2003; Garcias-Bonet and Duarte
194 2017). Briefly, the $\delta^{13}C$ of the CO_2 and CH_4 produced was extracted from the intercept of the
195 linear regression between the inverse of the gas partial pressure and the isotopic signature.

196

197 ## 3 Results

198 The mean (± SE) diel CO_2 and CH_4 emission rates for the seven sites were 372 ± 1309 µmol CO_2
199 m^{-2} d^{-1} and 5.6 ± 1.6 µmol CH_4 m^{-2} d^{-1} , respectively. We observed high variability among the
200 seven mangrove forest sites studied, with net CO_2 and CH_4 diel emission rates ranging from -
201 3452 to 7500 µmol CO_2 m^{-2} d^{-1} and from 0.9 to 13.3 µmol CH_4 m^{-2} d^{-1}, respectively (Table 1).

202 Mangrove sediments absorbed CO_2 during daytime and emitted CO_2 during night time, with
203 means (± SE) of -54.6 ± 37 µmol CO_2 m^{-2} d^{-1} and 86 ± 120 µmol CO_2 m^{-2} d^{-1} respectively (Table
204 1, Fig. 2). However, in three out of seven sites, heterotrophic activities outbalanced
205 photosynthesis on a 24h basis. At two sites, S3 and S6, we found an increase of the CO_2
206 emissions between day and night, contradictory to the classical daytime primary production–
207 night-time respiration pattern, possibly indicative of a light mediated increase of heterotrophic
208 processes.

209 Methane emissions did not show circadian patterns with linear increases in CH_4 concentration in
210 our incubations (Fig. 2) and with similar light and dark rates (0.26 ± 0.08 and 0.21 ± 0.07 µmol
211 CH_4 m^{-2} h^{-1} (mean ± SE), respectively (Table 1)). In terms of total GHG contribution, the mean
212 CO_2-equivalents (CO_2e) emission was 564 ± 1284 µmol CO_2e m^{-2} d^{-1} (mean ± SE); mangrove
213 sediments were net emitters of CO_2e in three out of seven sites (Table 1), and in five out of seven
214 mangrove stands sampled, CH_4 was the main source of CO_2e to the atmosphere.

215 While no overall trend was revealed through the relationship between day and night fluxes for
216 CO_2 and CH_4 (Fig. 3), consistencies are evident at specific mangrove stations. For example,
217 night CO_2 emissions are clearly visible at S2, while S3 appears to emit CO_2 during daylight
218 hours. No relationship was apparent between GHG fluxes and the densities of organic carbon or

nitrogen in the sediment. There was no discernible trend between gas fluxes and chlorophyll *a* content in surface sediments.

The isotopic signatures of the produced CO_2 ($\delta^{13}C\text{-}CO_2$) ranged from -11.21 to -25.72 ‰ as derived from keeling plots (Fig. 4, Table 1). The $\delta^{13}C\text{-}CO_2$ was similar for almost all stations, with the exception of S3 that had a $\delta^{13}C\text{-}CO_2$ of -25.72 ‰. The isotopic composition of the produced CH_4 ($\delta^{13}C\text{-}CH_4$) ranged from -71.28 to -87.08 ‰, with a mean $\delta^{13}C$ signature of -80.61 ‰ (Fig. 4, Table 1). The data set is available from Sea et al. (2018).

4 Discussion

The CO_2 and CH_4 emissions reported in this study show that Red Sea mangrove sediments can act as a source of GHG to the atmosphere. Values reported from this study fall within previously reported ranges for both CH_4 and CO_2, but maximum CH_4 and CO_2 flux rates in the Red Sea are over 10 to 100 fold below those reported elsewhere (Table 2). The variability in GHG emission rates reported here could be attributed to spatial differences, as cores were taken from different parts of each forest. Previous studies report significant discrepancies in emission rates in fringe versus forest positions (Allen et al., 2007), although this is likely to be a minor source of variability provided the narrow belt Red Sea mangroves typically form, about 30 m, due to the restricted tidal range of about 0.6 m in this region.

The uniformity of day and night emission rates for CH_4 we observed in Red Sea mangrove stands is consistent with previous work reporting that emission rates for CH_4 do not vary significantly during light and dark hours in mangrove forests (Allen et al., 2007). It has been suggested instead that variables such as sediment temperature are more significant in their contributions to emission rates (Allen et al., 2007; Allen et al., 2011). Indeed, seasonal studies of longer duration have reported increased emission rates during warmer seasons (Chen et al., 2016; Livesley and Andrusiak, 2012). Methane concentrations typically remain low due to anaerobic methane oxidation processes that take place near sediment surfaces (Kristensen et al., 2008a), consistent with the low CH_4 emission rates from Red Sea mangrove sediments observed here. Additionally, environments of high salinity like the Red Sea have been associated with decreased

247 CH_4 emissions, as sulfate-reducing bacteria are thought to outcompete methanogens
248 (Poffenbarger et al., 2011).

249 There were no relationships between GHG fluxes and sediment properties, such as chlorophyll *a*,
250 nitrogen density, and organic carbon density, suggesting that other factors have greater influence
251 on GHG flux rates in this region. Since mangroves can receive large contributions of organic
252 carbon from other sources (Newell et al., 1995), such as algal mats, seagrass and seaweed, the
253 examination of the isotopic composition of emitted carbon provides insights into the origin of the
254 organic carbon supporting GHG fluxes in mangrove sediments. The isotopic signature of the
255 CO_2 ($\delta^{13}C\text{-}CO_2$) produced by mangrove sediments in four out of the five mangrove stands with
256 available isotopic data was heavier (from -11.2 ± 0.6 to -15.9 ± 1.1 ‰ (Table 1)) than the
257 isotopic signature of mangrove tissues, suggesting the decomposition of organic matter from
258 mixed sources (Kennedy et al. 2010). Specifically, the isotopic signature of the mangroves found
259 in the central Red Sea has been recently reported as $\delta^{13}C_{leaves}$ = -26.98 ± 0.15 ‰, $\delta^{13}C_{stems}$ = -
260 25.75 ± 0.16 ‰ and $\delta^{13}C_{roots}$ = -24.90 ± 0.17 ‰ for mangrove leaves, stems and roots while the
261 mean isotopic signature of other primary producers in the central the Red Sea has been reported
262 as $\delta^{13}C_{seaweed}$ = -12.8 ± 0.5 ‰ and $\delta^{13}C_{seagrass}$ = -8.2 ± 0.2 ‰ for seaweed and seagrass tissues,
263 respectively (Almahasheer et al. 20170). However, in one mangrove stand (S3) the $\delta^{13}C\text{-}CO_2$
264 was much lighter (-25.72 ± 0.21 ‰), indicative of mangrove tissues. Thus, according to the
265 isotopic signature, the CO_2 produced in mangrove sediments would be supported by mangrove
266 biomass in only one mangrove stand out of the five sampled sites with available isotopic data.
267 Moreover, the mean isotopic signature of the CH_4 produced in mangrove sediments ($\delta^{13}C\text{-}CH_4$ =
268 -80.6 ‰) confirms its biogenic origin, which normally ranges from -40 to -80 ‰, depending on
269 the isotopic signature of the organic compounds being biologically decomposed (Reeburgh,
270 2014). The lowest $\delta^{13}C\text{-}CH_4$ was detected in S3, coinciding with the lowest $\delta^{13}C\text{-}CO_2$ value,
271 suggesting that the organic matter being decomposed by methanogens came from mangrove
272 tissues as well.

273 Interestingly, the mangrove with the lightest $\delta^{13}C\text{-}CO_2$ and $\delta^{13}C\text{-}CH_4$ (S3), showed the lowest
274 daily CO_2 flux (-1524 ± 686 µmol CO_2 m^{-2} d^{-1}) but the highest CH_4 emission rate (13.3 ± 9.5
275 µmol CH_4 m^{-2} d^{-1}), compared to the fluxes detected in the rest of mangrove stands with available
276 isotopic data. Part of the variability in the CO_2 (R^2=0.42) and CH_4 (R^2=0.40) emission rate seems

277 to be explained by the origin of the organic matter being decomposed, estimated here as the
278 $\delta^{13}C\text{-}CO_2$ and $\delta^{13}C\text{-}CH_4$. Organic matter with lighter isotopic composition would enhance CO_2
279 emissions; whereas organic matter with heavier isotopic composition would enhance CH_4
280 emissions (Fig. 5), suggesting a different preferential use of organic matter by different microbial
281 groups in mangrove sediments. This corroborates the importance of the origin of the organic
282 carbon stored in mangrove sediments on their GHG emissions.

283 This study is first in reporting CO_2 and CH_4 fluxes from Red Sea mangrove sediments,
284 contributing to the scant data on arid mangrove systems (Atwood et al. 2017, Almahasheer et al.
285 2017) essential to establish a solid baseline on GHG emissions for future studies. Seasonal
286 variation should be considered in future studies on GHG emissions by Red Sea mangroves to
287 better determine annual emission rates from this system, which reaches some of the warmest
288 temperatures experienced by mangrove forests worldwide. Similarly, a wider spatial coverage
289 within the mangrove forest should be considered to confidently determine net GHG fluxes that
290 can be upscaled to the entire stock of Red Sea mangroves. While many studies use the static
291 chamber technique to determine concentrations of methane and carbon dioxide, the highly
292 sensitive CRDS was able to detect trace gases at very low concentrations, making this device
293 useful in future flux studies. However, it is recognized that inherent differences in reported
294 emissions exist as a result of two different sampling techniques used in this study. Establishing a
295 unified GHG sampling technique for mangrove sediments will aid future researchers in
296 establishing total carbon budgets and accurately informing policymakers of their findings.

297 Methane emission rates from Red Sea mangrove sediments, although quite low, become more
298 substantial when considered in terms of global warming potential. In this study, CH_4 was, despite
299 the comparatively low emission rates, the main source of CO_2e in the majority of sampled
300 mangroves, and therefore deserves careful monitoring in this region. Reported organic carbon
301 burial rates of Red Sea mangroves of 3.42 mmol C m^{-2} d^{-1} (Almahasheer et al. 2017), are 10
302 times larger than the combined average CO_2 and CH_4 emission rates reported here (0.37 mmol C
303 m^{-2} d^{-1}), identifying mangrove sediments as net carbon sinks. The balance is lower when
304 computed in terms of CO_2e, the relevant metric in terms of radiative forcing, but still resulted in
305 a net CO_2e removal rate of about 2.9 mmol C m^{-2} d^{-1} by Red Sea mangrove sediments. Whereas
306 our results show that, despite sizeable CH_4 and CO_2 emissions, Red Sea mangrove sediments are

net sinks for organic carbon; their contribution to climate change, by either promoting it or mitigating it is not reflected on this balance. The role of Red Sea mangrove sediments in climate change depends on the changes experienced. In contrast to mangrove forests elsewhere around the world, Red Sea mangroves are not in decline and, rather, have expanded 12% from the 120 Km^2 occupied in 1972 to 132 Km^2 in 2013 (Almhasheer et al. 2016). Hence, Red Sea mangroves would have had a modest, but measurable contribution to climate change mitigation. Moreover, protection measures and further reforestation efforts are being deployed along the Red Sea that will further expand the area of mangroves (Almhasheer et al. 2016). The rationale for conserving mangroves, in the climate change context, is not adequately represented by their net carbon sink capacity when undisturbed, but rather by the emissions resulting from their disturbance. Indeed, previous studies analyzing anthropogenic impacts on methane emission rates from mangrove sediments have shown that disturbance significantly increases methane emissions (Purvaja and Ramesh, 2001; Chen et al., 2011). This provides an additional rationale to conserve, and continue to expand, Red Sea mangroves.

Data availability. All data will be accessible in the repository Pangea pending manuscript acceptance.

Competing interests. The authors declare that they have no conflict of interest.

Author contribution

MAS, NG-B, VS and CMD designed the study. MAS and NG-B performed the measurements and calculations. MAS, NG-B, VS and CMD interpreted the results. All authors contributed substantially to the final manuscript.

Acknowledgements

This research was funded by King Abdullah University of Science and Technology (KAUST) through baseline funding to C.M.D. We thank D. Krause-Jensen, Nabeel Massoudi, and

Kimberlee Baldree for help during sampling, and the captain and crew of KAUST R/V Thuwal for support. M.A.S. was supported by King Abdullah University of Science and Technology through the VRSP program. We thank P. Carrillo de Albornoz for lab instrument support, and Mongi Ennasri for help with sediment analysis.

References

Allen, D. E., Dalal, R. C., Rennenberg, H., Meyer, R., L., Reeves, S., Schmidt, S.: Spatial and temporal variation of nitrous oxide and methane flux between subtropical mangrove sediments and the atmosphere, Soil Biology and Biochemistry, 39, 622-631, 2007.

Allen, D. E., Dalal, R.C., Rennenberg, H., and Schmidt, S.: Seasonal variation in nitrous oxide and methane emissions from subtropical estuary and coastal mangrove sediments, Australia, Plant Biology, 13, 126-133, 2011.

Almahasheer, H., Aljowair, A., Duarte, C. M., Irigoien, X.: Decadal stability of Red Sea mangroves, Estuarine, Coastal and Shelf Science, 169, 164-172, 2016.

Almahasheer, H., Serrano, O., Duarte, C. M., Arias-Ortiz, A., Masque, P., and Irigoien, X.: Low carbon sink capacity of Red Sea mangroves, Scientific Reports, 7, 9700, doi:10.1038/s41598-017-10424-9, 2017.

Alongi, D. M.: Mangrove forests: Resilience, protection from tsunamis, and responses to global climate change, Estuarine, Coastal, and Shelf Science, 76, 1-13, 2008.

Alongi, D. M.: The energetics of mangrove forests, Springer Press, London, England, 2009.

Alongi, D. M.: Carbon sequestration in mangrove forests, Carbon Management, 3, 313-322, doi: 10.4155/cmt.12.20, 2012.

Alongi, D. M.: Carbon cycling and storage in mangrove forests, Annu. Rev. Mar. Sci., 6, 195-219, doi: 10.1146/annurev-marine-010213-135020, 2014.

Alongi, D. M., Pfitzner, J., Trott, L. A., Tirendi, F., Dixon, P., and Klumpp, D. W.: Rapid sediment accumulation and microbial mineralization in forests of the mangrove Kandelia candel in the Jiulongjiang Estuary, China, Estuarine, Coastal, and Shelf Science, 63, 605-618, 2005.

Atwood, T.B., Connolly, R.M., Almahasheer, H., Carnell, P., Duarte, C. M., Ewers, C., Irigoien, X., Kelleway, J., Lavery, P. S., Macreadie, P. I., Serrano, O., Sanders, C., Santos, I., Steven, A., and Lovelock, C. E.: Global patterns in mangrove soil carbon stocks and losses, Nature Climate Change, doi:10.1038/nclimate3326, 2017.

Chauhan, R., Datta, A., Ramanathan, A. L., Adhya, T. K.: Factors influencing spatio-temporal variation of methane and nitrous oxide emission from a tropical mangrove of eastern coast of India, Atmospheric Environment, 107, 95-106, 2015.

Chen, G., Tam, N. F. Y., Wong, Y. S., and Ye, Y.: Effect of wastewater discharge on greenhouse gas fluxes from mangrove soils, Atmospheric Environment, 45, 1110-1115, 2011.

Chen, G., Chen, B., Yu, D., Tam, N. F. Y., Ye, Y., and Chen, S.: Soil greenhouse gas emissions reduce the contribution of mangrove plants to the atmospheric cooling effect, Environmental Research Letters, 11, 1-10, doi:10.1088/1748-9326/11/12/124019, 2016.

Duarte, C. M., Losada, I. J., Hendriks, I. E., Mazarrasa, I., and Marbà, N.: The role of coastal plant communities for climate change mitigation and adaptation, Nature Climate Change, 3, 961-968, doi: 10.1038/NCLIMATE1970, 2013.

Donato, D. C., Kauffman, J. B., Murdiyarso, D., Kurnianto, S., Stidham, M., and Kanninen, M.: Mangroves among the most carbon-rich forests in the tropics, Nature Geoscience, 4, 293-297, doi: 10.1038/NGEO1123, 2011.

Garcias-Bonet, N. and Duarte, C. M.: Methane production by seagrass ecosystems in the Red Sea, Frontiers in Marine Science, 4, 340 doi: 10.3389/fmars.2017.00340, 2017.

Giri, C., Ochieng, E., Tieszen, L. L., Zhu, Z., Singh, A., Loveland, T., Masek, J., and Duke, N.: Status and distribution of mangrove forests of the world using earth observation satellite data, Global. Ecol. Biogeogr., 20, 154-159, 2011.

Kanninen, M.: Mangroves among the most carbon-rich forests in the tropics, Nature Geoscience, 4, 293-297, doi:10.1038/ngeo1123, 2011.

Kennedy, H., Beggins, J., Duarte, C. M., Fourqurean, J. W., Holmer, M., Marbà, N., and Middelburg, J. J.: Seagrass sediments as a global carbon sink: isotopic constraints, Global Biogeochemical Cycles, 24, GB4026, doi: 10.1029/2010GB003848, 2010.

Kristensen, E., Bouillon, S., Dittmar, T., and Marchand, C.: Organic carbon dynamics in mangrove ecosystems: A review, Aquatic Botany, 89, 201-219, doi:10.1016/j.aquabot.2007.12.005, 2008a.

Kristensen, E., Flindt, M. R., Ulomi, S., Borges, A. V., Abril, G., Bouillon, S.: Emissions of CO_2 and CH_4 to the atmosphere by sediments and open waters in two Tanzanian mangrove forests, Marine Ecology Progress Series, 370, 53-67, doi: 10.3354/meps07642, 2008b.

Livesley, S. J., and Andrusiak, S. M.: Temperate mangrove and salt marsh sediments are a small methane and nitrous oxide source but important carbon store, Estuarine, Coastal, and Shelf Science, 97, 19-27, 2012.

Myhre, G., Shindell, D., Bréon, F. M., Collins, W., Fuglestvedt, J., Huang, J., Koch, D., Lamarque, J. F., Lee, D., Mendoza, B., and Nakajima, T.: Anthropogenic and natural radiative forcing, Climate Change, 423, 2013.

Newell, R. I. E., Marshall, N., Sasekumar, A., Chong, V. C.: Relative importance of benthic microalgae, phytoplankton, and mangroves as sources of nutrition for penaeid prawns and other coastal invertebrates from Malaysia, Marine Biology, 123, 595-606, 1995.

Pataki, D., Ehleringer, J. R., Flanagan, L. B., Yakir, D., Bowling, D. R., Still, C. J., Buchmann, N., Kaplan, J. O., and Berry, J. A.: The application and interpretation of Keeling plots in terrestrial carbon cycle research, Global Biogeochemical Cycles, 17, 1022, doi: 10.1029/2001GB001850, 2013.

Poffenbarger, H. J., Needelman, B. A., and Megonigal, J. P.: Salinity influence on methane emissions from tidal marshes, Wetlands, 31, 831-842, doi: 10.1007/s13157-011-0197-0, 2011.

409 Purvaja, R. and Ramesh, R.: Human impacts on methane emission from mangrove ecosystems in
410 India, Regional Environmental Change, 1, 86-97, doi: 10.1007/PL00011537, 2000.

411 Purvaja, R. and Ramesh, R.: Natural and anthropogenic methane emission from wetlands of
412 south India, Environmental Management, 27, 547-557, doi: 10.1007/s002670010169, 2001.

413 Reeburgh, W. S.: Global Methane Biogeochemistry Treatise on Geochemistry (Second Edition),
414 Holland, H. D., and Turekian, K. K., Oxford, Elsevier, 71-94, 2014.

415 Sea, M. A., Garcias-Bonet, N., Saderne, V., and Duarte, C. M.: Data set on methane emissions
416 from Red Sea mangrove sediments. Pangea DOI: [data set will be published in the Pangea open
417 data repository at the acceptance of paper], 2018.

418 Soetaert, K., Petzoldt, T., and Meysman, F.: Marelac: A tool for aquatic sciences (R package),
419 available at: https://cran.r-project.org/web/packages/marelac/marelac.pdf, 2016.

420 Thom, M., Bosinger, R., Schmidt, M., and Levin, I.: The regional budget of atmospheric
421 methane of a highly populated area, Chemosphere, 26, 143-160, doi: 10.1016/0045-
422 6535(93)90418-5, 1993.

423 Wiesenburg, D. A. & Guinasso, N. L.: Equilibrium solubilities of methane, carbon monoxide,
424 and hydrogen in water and sea water, Journal of Chemical and Engineering Data, 24, 356-360,
425 1979.

426 Wilson, S. T., Böttjer, D., Church, M. J., and Karla, D. M.: Comparative assessment of nitrogen
427 fixation methodologies, conducted in the oligotrophic north Pacific Ocean, Applied and
428 Environmental Microbiology, 78, 6516-6523, 2012.

Biogeosciences Discuss., https://doi.org/10.5194/bg-2018-37
Manuscript under review for journal Biogeosciences
Discussion started: 31 January 2018

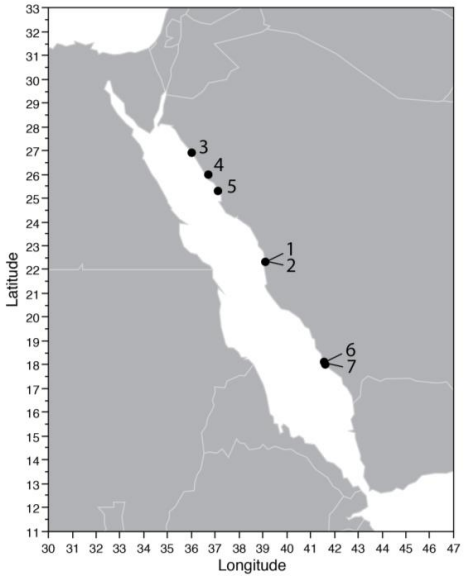

429

430 **Fig. 1.** Mangrove stands sampled along the Saudi coast of the Red Sea. Numbers indicate
431 positions of sampling sites from this study. S1 and S2: King Abdullah University of Science and
432 Technology; S3: Duba; S4 and S5: Al Wahj; S6 and S7: Farasan Banks.

433

434

435

436

437

438

Biogeosciences Discuss., https://doi.org/10.5194/bg-2018-37
Manuscript under review for journal Biogeosciences
Discussion started: 31 January 2018

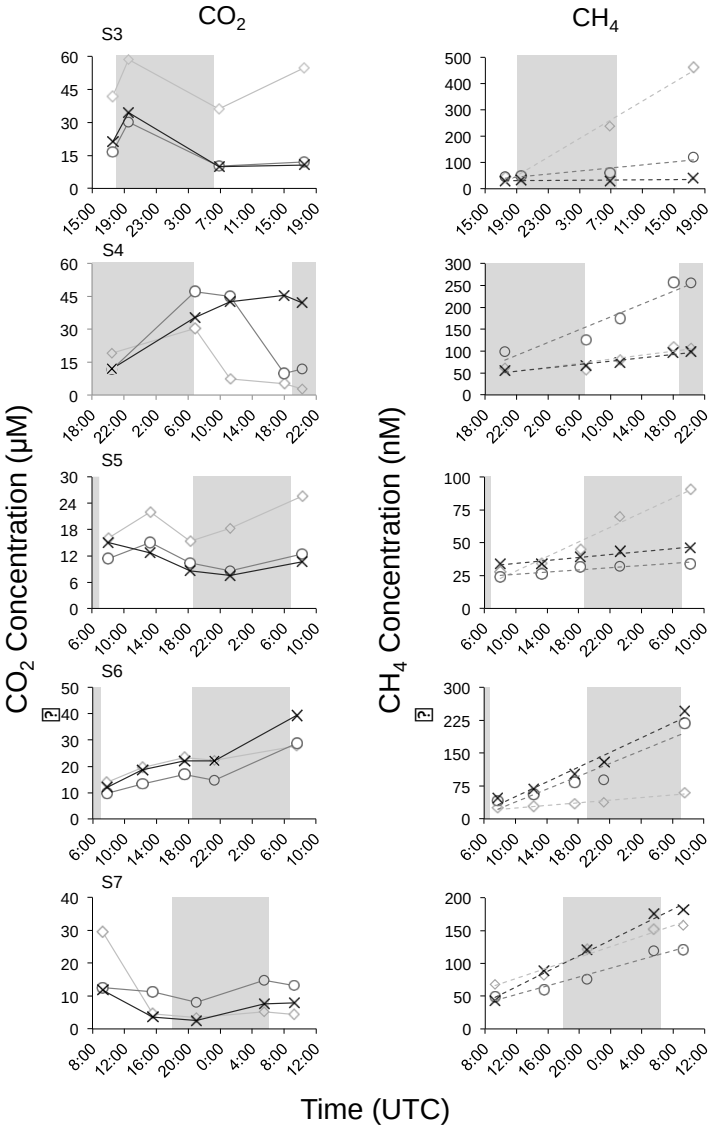

439

440 **Fig. 2.** Change in CO_2 (left panels) and CH_4 (right panels) concentrations over time in triplicated
441 mangrove sediment cores from mangrove stations S3-S7. Shaded areas represent night time and
442 each replicate is coded by different symbols.

443

Biogeosciences Discuss., https://doi.org/10.5194/bg-2018-37
Manuscript under review for journal Biogeosciences
Discussion started: 31 January 2018

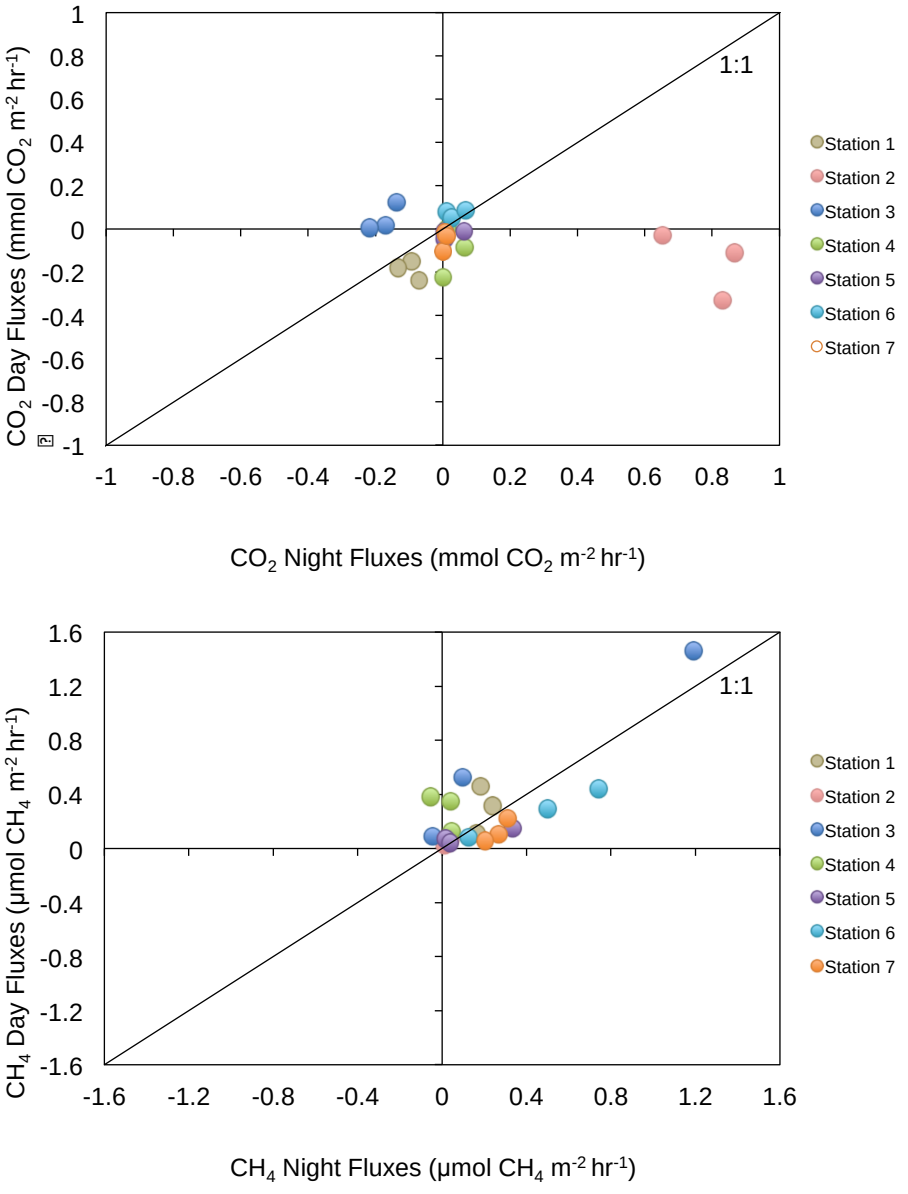

444

445 **Fig. 3.** Relationship between day and night fluxes for CO_2 (top panel) and CH_4 (bottom panel) at
446 all mangrove stations.

Biogeosciences Discuss., https://doi.org/10.5194/bg-2018-37
Manuscript under review for journal Biogeosciences
Discussion started: 31 January 2018

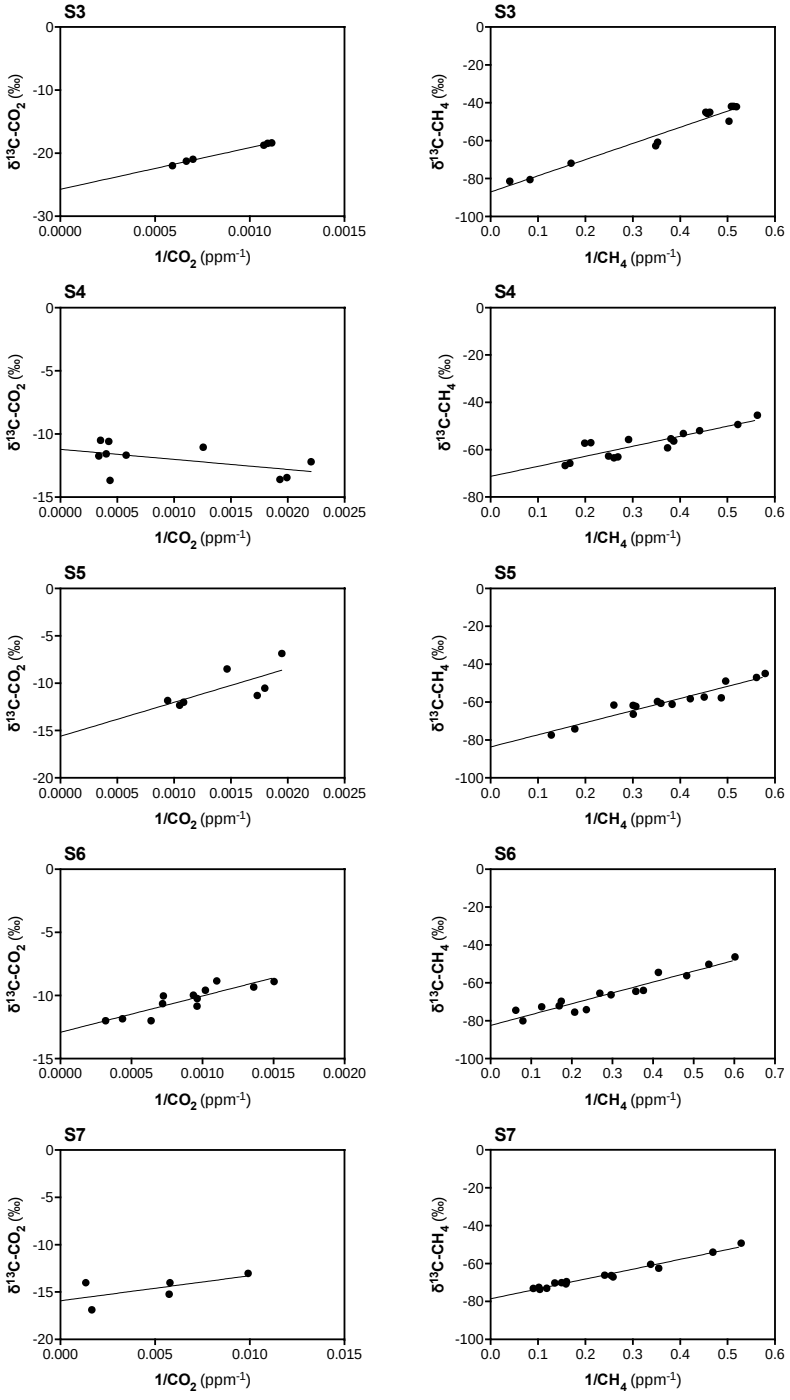

447

Biogeosciences Discuss., https://doi.org/10.5194/bg-2018-37
Manuscript under review for journal Biogeosciences
Discussion started: 31 January 2018

448 **Fig. 4.** Keeling plots for mangrove stations S3-S7, showing the linear regression of the inverse of
449 CO_2 concentration (left panels) and CH_4 concentration (right panels) versus $\delta^{13}C–CO_2$ and $\delta^{13}C–$
450 CH_4. Y-intercepts were used to estimate the isotopic signatures of produced gases.

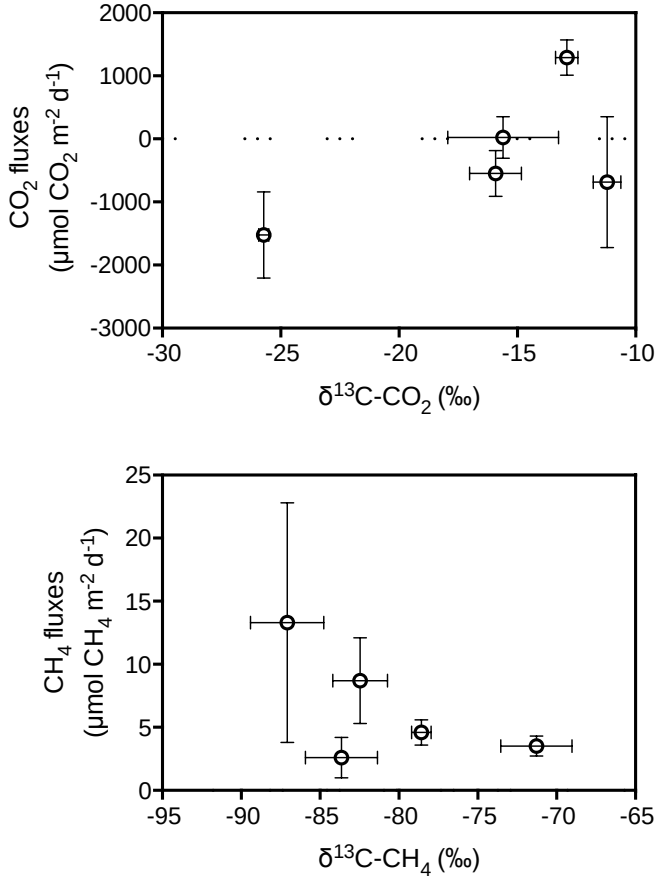

451

452 **Fig. 5.** Relation between the carbon isotopic signature of the produced CO_2 ($\delta^{13}C–CO_2$) and CO_2
453 fluxes (top panel) and carbon isotopic signature of the produced CH_4 ($\delta^{13}C–CH_4$) and the CH_4
454 fluxes (bottom panel) in Red Sea mangroves. Error bars indicate standard error of the mean.

455

456

Biogeosciences Discuss., https://doi.org/10.5194/bg-2018-37
Manuscript under review for journal Biogeosciences
Discussion started: 31 January 2018

Table 1. Summary of greenhouse gas fluxes and sediment characteristics from studied mangrove forests. CH_4 fluxes in brackets represent CO_2 equivalents in terms of global warming potential for a time horizon of 100 years (GWP_{100}), taking into account climate-carbon feedback as suggested by the AR5 of IPCC (Myhre et al., 2013). Data represent the mean ± SEM and nd means no data available.

Station	CO_2 Day Flux ($\mu mol\ m^{-2}\ hr^{-1}$)	CH_4 Day Flux ($\mu mol\ m^{-2}\ hr^{-1}$)	CO_2 Night Flux ($\mu mol\ m^{-2}\ hr^{-1}$)	CH_4 Night Flux ($\mu mol\ CH_4\ m^{-2}\ hr^{-1}$)	Daily CO_2 Flux ($\mu mol\ m^{-2}\ d^{-1}$)	Daily CH_4 Flux ($\mu mol\ m^{-2}\ d^{-1}$)	$\delta^{13}C$-CO_2 (‰)	$\delta^{13}C$-CH_4 (‰)	Nitrogen Density ($mg\ cm^{-3}$)	C_{org} Density ($mg\ cm^{-3}$)	Chl *a* ($\mu g\ Chl\ a\ g^{-1}_{sediment}$)
1	-188 ± 25	0.30 ± 0.17 [10.2]	-99 ± 18	0.19 ± 0.04 [6.46]	-3452 ± 271	5.9 ± 1.3 [201]	nd	nd	nd	nd	nd
2	-157 ± 89	0.05 ± 0.02 [1.7]	782 ± 66	0.03 ± 0.01 [1.02]	7500 ± 894	0.9 ± 0.25 [31]	nd	nd	nd	nd	nd
3	49 ± 37	0.69 ± 0.4 [23.46]	-176 ± 23	0.42 ± 0.39 [14.28]	-1524 ± 686	13.3 ± 9.5 [452]	-25.7 ± 0.2	-87.1 ± 2.3	1.03 ± 0.05	13.33 ± 1.01	nd
4	-86 ± 79	0.28 ± 0.1 [9.52]	29 ± 19	0.01 ± 0.03 [0.34]	-684 ± 1038	3.5 ± 0.8 [119]	-11.1 ± 0.6	-71.3 ± 2.3	0.80 ± 0.03	8.98 ± 0.86	1.02 ± 0.05
5	-22 ± 11	0.09 ± 0.03 [3.06]	24 ± 20	0.13 ± 0.10 [4.42]	23 ± 331	2.6 ± 1.6 [88]	-15.6 ± 2.3	-83.6 ± 2.3	1.12 ± 0.05	13.34 ± 0.98	1.03 ± 0.04
6	73 ± 10	0.27 ± 0.10 [9.18]	35 ± 17	0.45 ± 0.18 [15.30]	1289 ± 280	8.7 ± 3.4 [296]	-12.9 ± 0.5	-82.5 ± 1.7	1.51 ± 0.14	10.58 ± 0.82	0.43 ± 0.14
7	-51 ± 28	0.13 ± 0.05 [4.42]	5 ± 3	0.26 ± 0.03 [8.84]	-547 ± 363	4.6 ± 1.0 [156]	-15.9 ± 1.1	-78.6 ± 0.6	3.30 ± 0.55	33.43 ± 6.69	1.86 ± 0.12

Biogeosciences Discuss., https://doi.org/10.5194/bg-2018-37
Manuscript under review for journal Biogeosciences
Discussion started: 31 January 2018

Table 2. Comparison of GHG fluxes from global mangrove forests and Red Sea mangroves. Literature values converted from reported form for comparison purposes.

		CO_2 ($mmol\ m^{-2}\ d^{-1}$)		CH_4 ($\mu mol\ m^{-2}\ d^{-1}$)	
		Minimum	Maximum	Minimum	Maximum
Kristensen, 2008a	Global	2	373	0	5000
Kristensen, 2008b	Tanzania	28	115	0	87.6
Livesley & Andrusiak, 2012	Australia	50	150	50	749
Alongi, 2005	China	17	121	5	66
Alongi, 2014	Global	49	69	0	5100
Chen, 2016	China	-16.9	279.2	-2.1	8015.1
Allen, 2007	Australia	-	-	4.5	25974
Allen, 2011	Australia	-	-	70.3	2348
Chuang, 2015	Mexico	-	-	12	11000
This Study	Red Sea	-3.5	7.5	0.9	13.3